Abstract

Keywords:

1. Mean power (Have to use a better title than this)

Mass ratio (m^*) and damping ratio(ζ) was treated as two different variables in the presentation of data. Fig. 1 and 2 shows the mean power against U^* at different ζ and m^*. The data in Fig 1 seems to agree qualitatively with Barrero-Gil et al. (2010) where the peak power was shifting when the damping ratio increased. An interesting observation is that the peak power remains to be constant regardless of the damping ratio where Barrero-Gil et al. (2010) also observed and concluded that the maximum efficiency attainable does not depend the $m^*\zeta$ parameter. A similar observation was made when m^* was increased (Fig.2). However, the peak power at $m^* = 20$ was lesser than the other mass ratios ($m^* = 30, 40, 60$) which produced the same peak mean power. This may be due to the effect of shedding. Joly et al. (2012) an influence of vortex shedding on galloping amplitude at low mass ratios. The data obtained using Parkinson and Smith (1964) C_y curve shows a similar pattern (Fig.5) where a common maximum power could be observed. Hysteresis could be observed in the power curves. The mean power data at different damping ratios could be collapsed by changing the independent variable form U^* to the damping factor $= \frac{4\pi\zeta m^*}{U^*}$ Fig.3. This phenomenon could also be observed when the mean power data at different mass ratios plotted in the earlier mentioned independent variable.

An explanation for this could be provided using an energy point of view. The power generally could be expressed as the product of force and velocity. Therefore the product of the force exerted by C_y and the velocity of the body $\dot{y}$, could be expressed as the power transfer from fluid to body (disregarding minor losses). On the other hand by using the term $(c\dot{y})\dot{y}$ the dissipated power due to mechanical damping of the system could be obtained.

As an example time histories of both dissipated power and the transferred power are presented in 3 different reduced velocities $U^* = 165, 95, 400$ (At regions where the mean power rises, peaks and falls respectively.) at Re 165 ζ 0.1 and m^* 40. (Fig6, 7, and 8). For the ease of reference let the transferred power be P_t and the dissipated power due to the damping of the mechanical system be P_d. It is to be noted that the shedding term is equated to zero in order to get a clear signal of galloping and as well as the shedding does not contribute to the mean power.

The Force exerted on the body (due to C_y) seems to be in phase with the motion of the body $\dot{y}$, Fig.6 at $U^* = 90$. At the region where the mean power becomes maximum where $U^* = 165$ there is an indication of the force and the motion go out of phase from the dip in

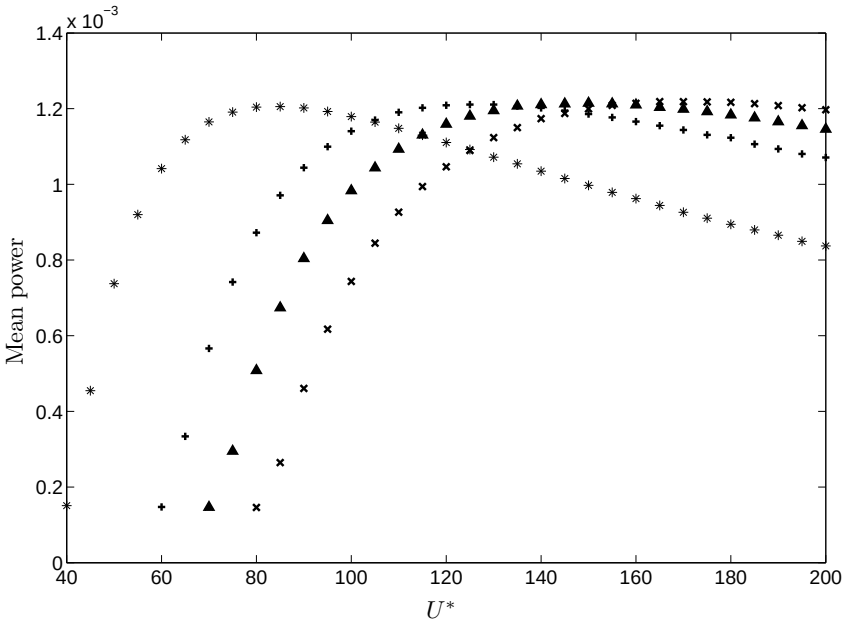

Figure 1: Mean power vs. reduced velocity at different damping ratios at $m^* = 20$. ✳ $\zeta = 0.1$, ✚ $\zeta = 0.15$, ▲ $\zeta = 0.175$ and ✖ $\zeta = 0.2$, at Re = 165.

Fig.2. At $U^* = 400$ Fig.8 which is in the region where the power decreases with increasing U^*, it could be seen that P_t becomes negative at a certain point in time which implies that the energy transfer occurs from body to fluid. This is due to the fact that the damping factor is small with increasing reduced velocities and therefore the energy transferred from fluid to body could not be dissipated solely by the mechanical damping.

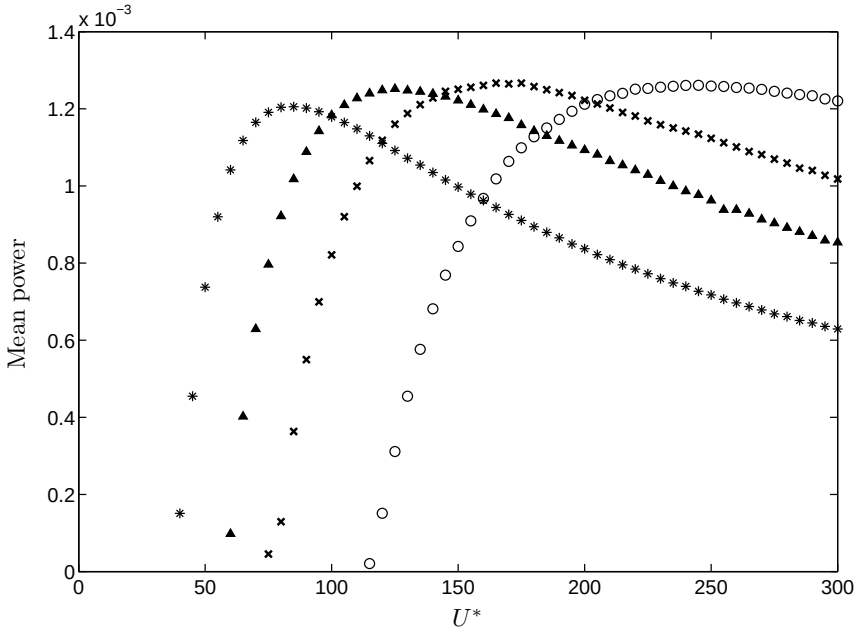

Figure 2: Mean power vs. U^* at different m^* $\zeta = 0.1$ ($\ast$ $m^* = 20$, $\blacktriangle$ $m^* = 30$, $\times$ $m^* = 40$ and $\circ$ $m^* = 60$,, at Re = 165)

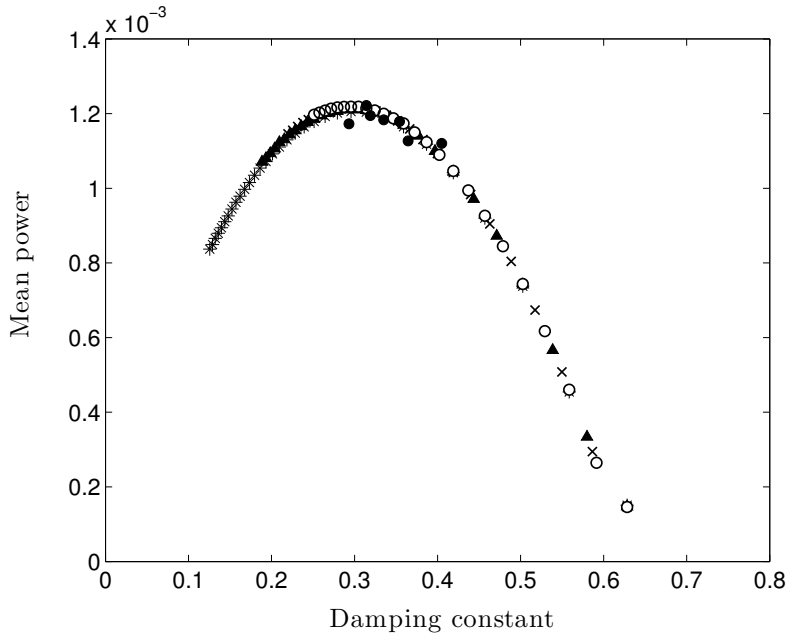

Figure 3: Mean power vs. damping constant at $m^* = 20$. $\ast$ $\zeta = 0.1$, $\blacktriangle$ $\zeta = 0.15$, $\times$ $\zeta = 0.175$ and $\circ$ $\zeta = 0.2$ and $\bullet$ FSI data at Re = 165

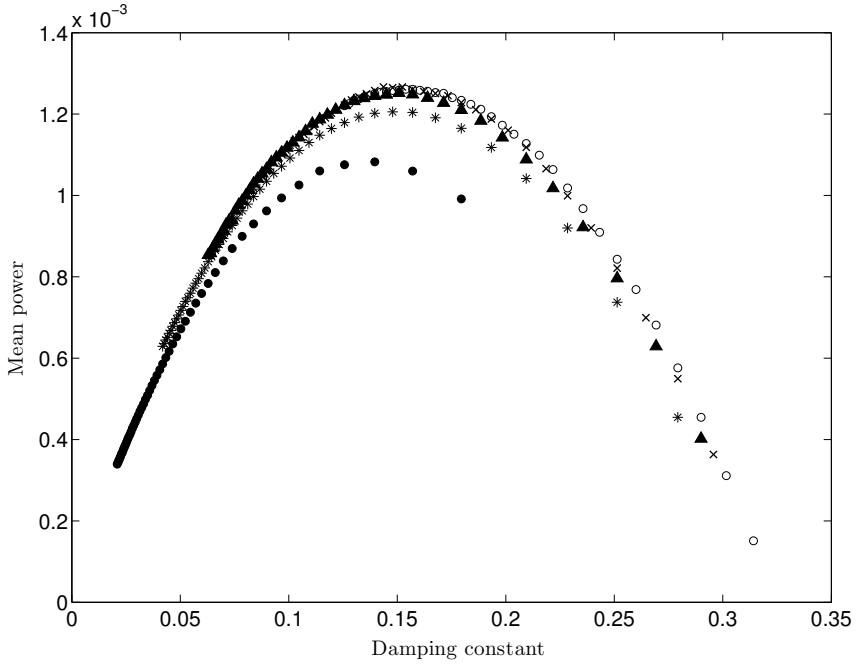

Figure 4: Mean power vs. damping ratio at different m^* $\zeta = 0.1$ (,● $m^* = 10$,✳ $m^* = 20$, ▲ $m^* = 30$, × $m^* = 40$ and ◯ $m^* = 60$, at Re = 165)

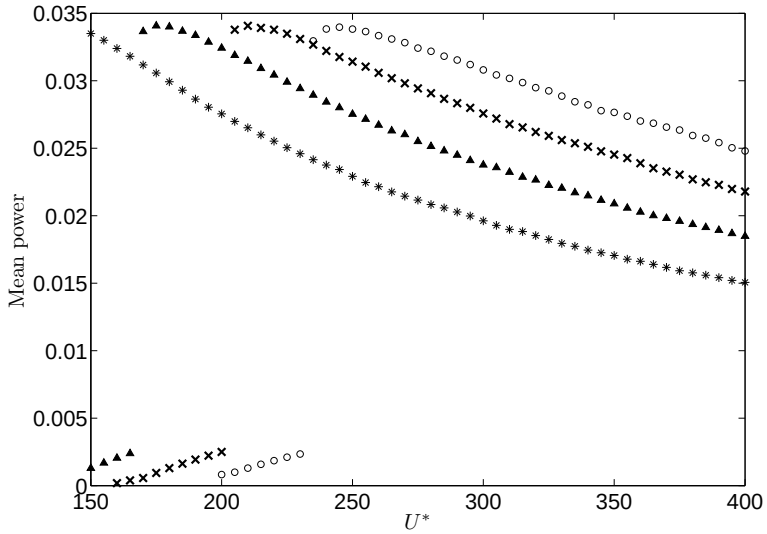

Figure 5:

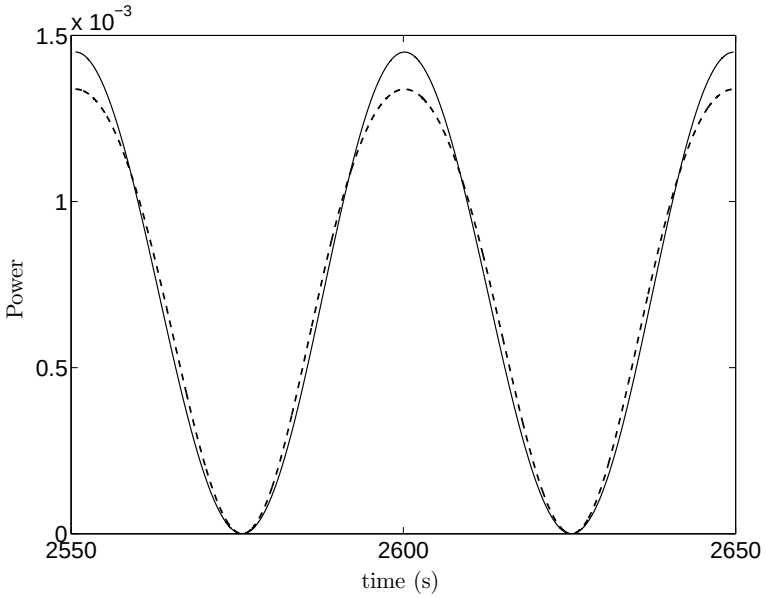

Figure 6:

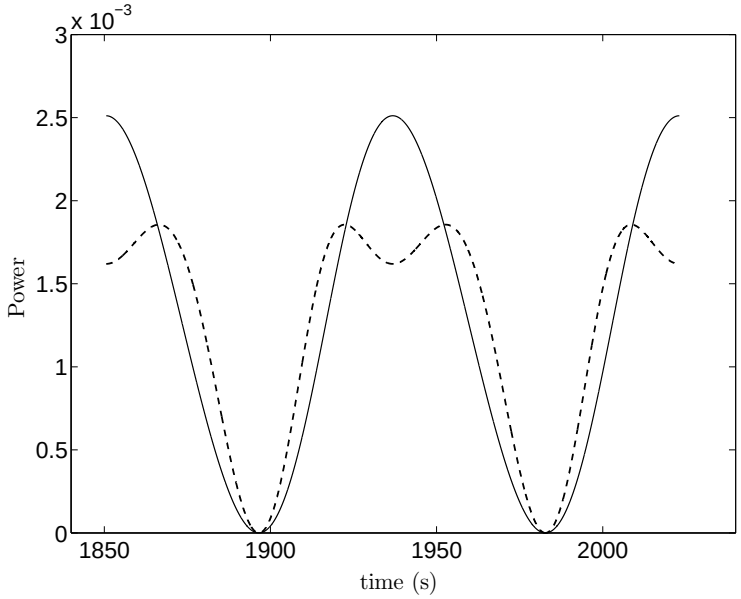

Figure 7:

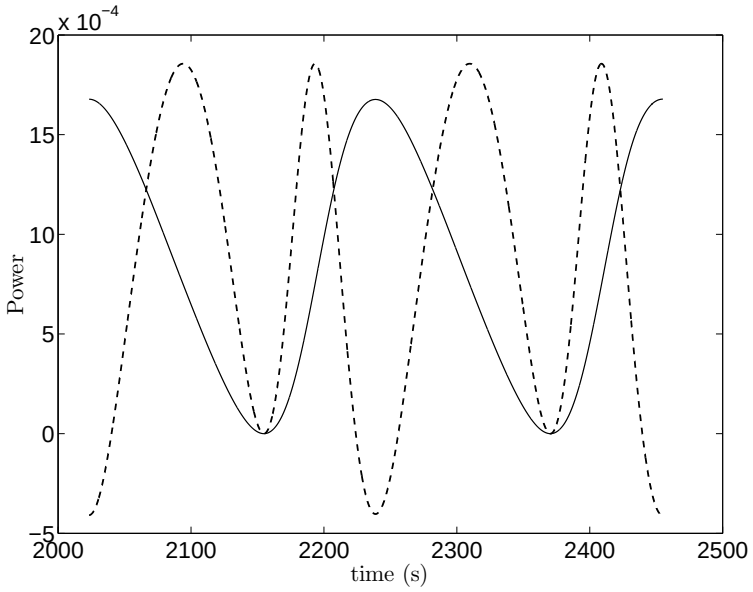

Figure 8:

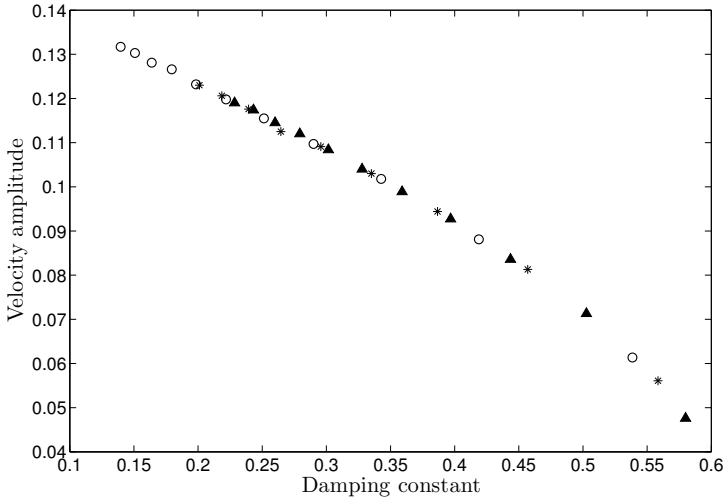

Figure 9: Velocity amplitude vs. damping constant at $m^* = 20$. $\circ$ $\zeta = 0.075$, $\ast$ $\zeta = 0.1$, $\blacktriangle$ and $\zeta = 0.15$, at Re = 165

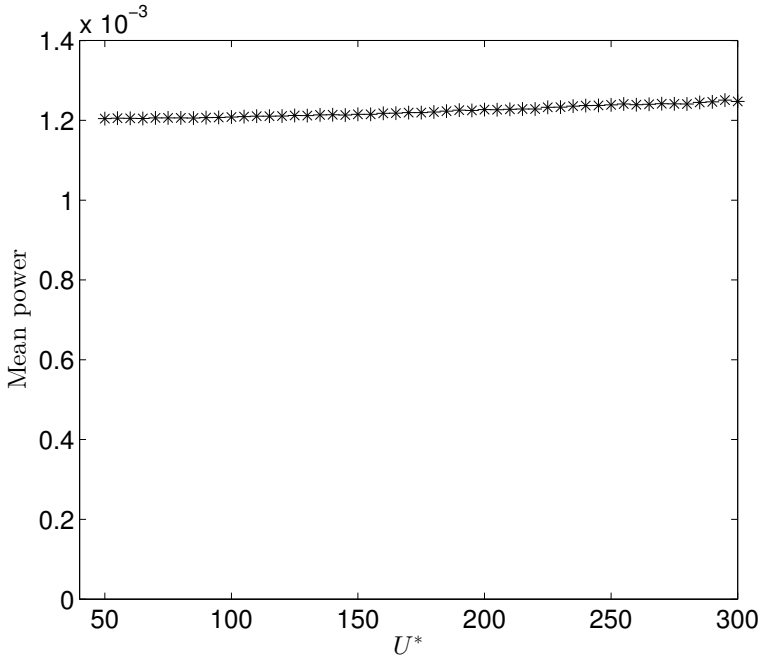

Figure 10: Plot of mean power at damping factor = 2.99

References

Barrero-Gil, A., Alonso, G., Sanz-Andres, A., Jul. 2010. Energy harvesting from transverse galloping. Journal of Sound and Vibration 329 (14), 2873–2883.

Bernitsas, M. M., Raghavan, K., Ben-Simon, Y., Garcia, E. M. H., 2008. VIVACE (Vortex Induced Vibration Aquatic Clean Energy): A new concept in generation of clean and renewable energy from fluid flow. Journal of Offshore Mechanics and Arctic Engineering 130 (4), 041101–15.

Den Hartog, J. P., 1956. Mechanical Vibrations. Dover Books on Engineering. Dover Publications.

Glauert, H., 1919. The rotation of an aerofoil about a fixed axis. Tech. rep., Advisory Committee on Aeronautics R and M 595. HMSO, London.

Joly, A., Etienne, S., Pelletier, D., Jan. 2012. Galloping of square cylinders in cross-flow at low Reynolds numbers. Journal of Fluids and Structures 28, 232–243.

Lee, J., Bernitsas, M., Nov. 2011. High-damping, high-Reynolds VIV tests for energy harnessing using the VIVACE converter. Ocean Engineering 38 (16), 1697–1712.

Ng, Y., Luo, S., Chew, Y., Jan. 2005. On using high-order polynomial curve fits in the quasi-steady theory for square-cylinder galloping. Journal of Fluids and Structures 20 (1), 141–146.
URL http://linkinghub.elsevier.com/retrieve/pii/S0889974604001215

Païdoussis, M., Price, S., de Langre, E., 2010. Fluid-Structure Interactions : Cross-Flow-Induced Instabilities. Cambridge University Press.

Parkinson, G. V., Smith, J. D., 1964. The square prism as an aeroelastic non-linear oscillator. The Quarterly Journal of Mechanics and Applied Mathematics 17 (2), 225–239.

Raghavan, K., Bernitsas, M., Apr. 2011. Experimental investigation of Reynolds number effect on vortex induced vibration of rigid circular cylinder on elastic supports. Ocean Engineering 38 (5-6), 719–731.

Raghavan, K., Bernitsas, M. M., Maroulis, D. E., 2009. Effect of Bottom Boundary on VIV for Energy Harnessing at $8 \times 10^3 < Re < 1.5 \times 10^5$. Journal of Offshore Mechanics and Arctic Engineering 131 (3), 031102.

Sheard, G. J., Fitxgerald, M. J., Ryan, K., Jun. 2009. Cylinders with square cross-section: wake instabilities with incidence angle variation. Journal of Fluid Mechanics 630, 43.

Tong, X., Luo, S., Khoo, B., Oct. 2008. Transition phenomena in the wake of an inclined square cylinder. Journal of Fluids and Structures 24 (7), 994–1005.
URL http://linkinghub.elsevier.com/retrieve/pii/S088997460800025X